ELSEVIER

Journal of Power Sources 83 (1999) 162–169

JOURNAL OF POWER SOURCES

www.elsevier.com/locate/jpowsour

Multi electrode prismatic power prototype carbon/carbon supercapacitors

L. Bonnefoi [a], P. Simon [a,*], J.F. Fauvarque [a], C. Sarrazin [b], J.F. Sarrau [b], P. Lailler [b]

[a] *CNAM-Laboratoire d'Electrochimie Industrielle, 2, rue conté 75003 Paris, France*
[b] *EXIDE-CEAC, Departement Recherche, 5-7, allée des Pierres Mayettes, 92636 Genneviliers cedex, France*

Received 18 January 1999; received in revised form 1 April 1999; accepted 27 April 1999

Abstract

This work describes the fabrication and the characterization of low-cost 2 V carbon/carbon power supercapacitors. Each cell had a volume of 100 cm^3. Three 2 V-supercapacitors were assembled and tested under different currents and at different temperatures. The measurements have shown a specific power of 1.1 kW/kg, a volumetric capacitance of 25 F/cm^3 per electrode and a time constant of 2 s.

Keywords: Double layer capacitor; Active material composition; Power capacitor; Low time constant

1. Introduction

Supercapacitors have been extensively studied for many years, since they are interesting for power applications such as mobile telecommunication, back up power for engines, starting and so on [1–4].

Three kinds of electrode materials can be used for supercapacitors: high surface area activated carbons, metal oxide and conducting polymers [5–7]. The objective of this work is to fabricate low-cost supercapacitors for automotive applications. To achieve this goal, it was decided to use high surface area activated carbons due to their low cost. In these types of supercapacitors, called Double Layer Capacitors (DLC), the energy is stored in the double layer formed near the carbon electrode surface, which must be as high as possible. Meanwhile, the resistivity increases with increasing the surface area and thus, it is important to adjust the surface area to minimize the resistance. The electrolyte may be aqueous or organic. The use of aqueous electrolytes allows to obtain a low series resistance for the supercapacitor, but limits its voltage to a value close to 1 V. In contrast, organic electrolytes allow the supercapacitor to reach 2 or 3 V however with a higher series resistance. The choice of the electrolyte depends on the specific desired power and energy values.

The objectives of this work are to fabricate a 12 V Double Layer Capacitor by assembling 6 cells of 2 V each in series. This paper describes the fabrication of the 2 V cells.

2. Experimental

2.1. Electrodes

Norit SX Ultra activated carbon (1200 m^2/g, 80 F/g) was used as the active electrode material. An electronic conductor was added to the activated carbon in order to ensure good electronic conductivity. A mixture containing the activated carbon material and the electronic conductor was added to a solution of organic binder. After heating, the mixture was spread out on a nickel-foam current collectors. The electrodes were first heated in air and then under vacuum.

The electrolyte used was a solution of acetonitrile (ACN) containing 1.7 M NEt_4MeSO_3. This electrolyte has a good conductivity (20 mS/cm) and does not contain fluorine compounds.

2.2. Capacitance and resistance measurements

Cells were assembled in a prismatic way with a cellulosic separator in between. Supercapacitors were cycled

* Corresponding author. Tel.: +33-1-40-27-26-78; fax: +33-1-40-27-24-20; E-mail: simon@cnam.fr

0378-7753/99/$ - see front matter
PII: S0378-7753(99)00292-X

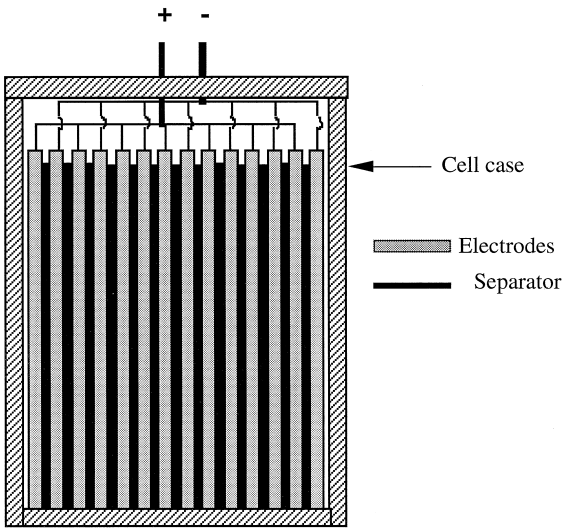

Fig. 1. Cross-section of the supercapacitor.

2000 × under constant current between 0 and 2.15 V using a Bitrode (time resolution: 1 s) and a Biologic VMP (time resolution: 20 ms). The characteristics of the supercapacitors remained constant during these cycles. Capacitance was calculated from the slope of the $V(t)$ plot. Resistance measurements were calculated either using an Electrochemical Impedance Spectrometer Solartron Schlumberger 1255 (at 1000 Hz), or from the ohmic drop during cycling with the Bitrode or the VMP apparatus.

3. Results and discussion

3.1. Cell assembly

The inner dimensions (in cm) of the cell case are 4.7 × 1.8 × 8.5. Current collectors used in this work were nickel foam strips of 2 mm in thickness. These strips were pasted with the active material mixture of activated carbon, electronic conductor and organic binder. Electrodes were cut out of these strips. Nickel foil (200 μm thick and 3 cm long) was then soldered onto the top of the electrodes to be used as the end plates. The electrodes were then pressed in order to decrease their thickness and to enhance the contact between the active mass and the current collector. For a better control of the thickness, electrodes were laminated to achieve thicknesses between 450 and 850 μm.

Electrodes were soldered and placed in a polypropylene case. The top of the case was welded with hot polypropylene and then the case was filled with the electrolyte. Fig. 1 presents a cross-section of the cell.

Table 1
Characteristics of the supercapacitor SC#1 during cycling at constant current ($T = 25°C$)

I (A)	V_{dis} (V)	C (F)	R_{cycl} (mΩ)	$R_{1000\ Hz}$ (mΩ)
2	2.07	243	23	10.5
4	2.03	233	21.5	10.5
10	1.91	226	20.5	10.5

3.2. SC#1 cell tests

A first supercapacitor SC#1 was assembled. The electrode composition was 80% activated carbon, 15% electronic conductor, 5% Carboxymethylcellulose (CMC). This composition confers a good level of conductivity associated with a volumetric capacitance close to 23 F/cm^3 per

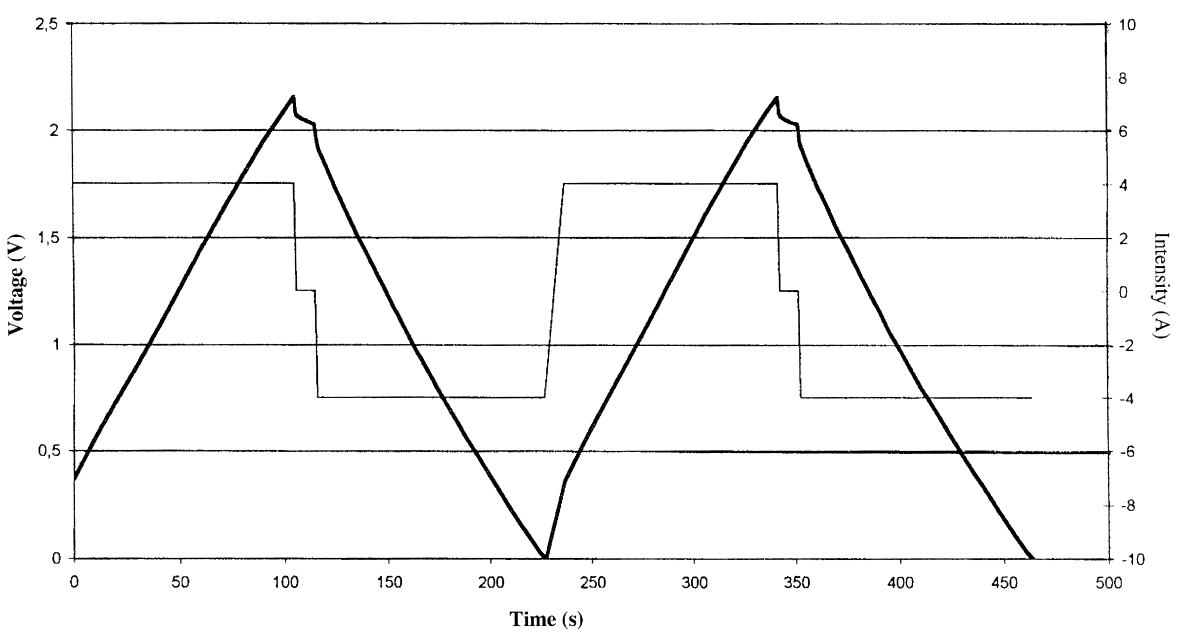

Fig. 2. Constant current charge–discharge cycles for the SC#1 cell. $I = 4$ A.

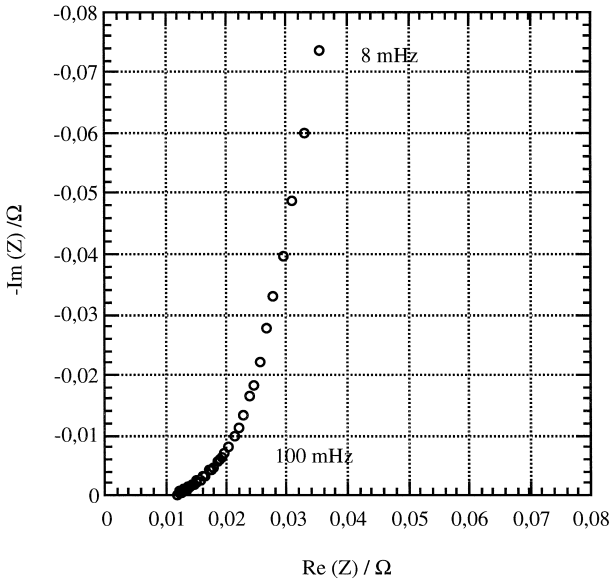

Fig. 3. Impedance spectrum of the SC#1 cell, between 2 kHz and 8 mHz.

electrode [8]. 20 electrodes were assembled (10 by polarity) to form a prismatic cell.

3.2.1. Constant current cycling

Fig. 2 shows cycling curves between 0 and 2.15 V at 4 A ($T = 25°C$) and Table 1 presents the characteristics of the cell. For this cell, the resistance was measured in two different ways. The first resistance noted R_{cycl} corresponds to that obtained during cycling. This resistance was calculated from the initial step voltage at the beginning of a charge–discharge cycle. This ohmic drop was not corrected for the capacitance voltage change (It/c) that occurs before the acquisition of the first data point (1 s) in the charge or discharge. The second value of the resistance at 1000 Hz is deduced from the impedance measurements carried out for each cell.

The capacitance was found to be equal to 243 F at 2 A, which corresponds to 75 F/g of activated carbon. This value is near the theoretical capacitance of the Norit SX Ultra (80 F/g), which shows that all the material is active. The volumetric capacitance of one electrode is 21 F/cm^3 including the current collector, which is a rather low value. The specific surface resistance calculated from the R_{cycl} data is 13 Ω cm^2. Significant improvements will have to be made to decrease this value.

The cycling of the supercapacitor up to 10 A shows that a small capacitance loss (6%) appears (Table 1), associated with a decrease of the resistance, but the general behavior is correct.

3.2.2. Impedance measurements

Fig. 3 presents the Nyquist plot of the SC#1 run in the 2 kHz and 8 mHz frequency range. The knee frequency appears at 100 mHz, this being a rather low value [9]. In theory, this frequency limits two different behaviors of the supercapacitor, i.e., above the knee frequency the real part of the impedance (the resistance) is frequency dependent, while below this value, the resistance changes weakly with frequency and the supercapacitor behavior tends to approach that of a pure capacitance. In our case, the capacitive behavior below 100 mHz is not very pronounced, as the slope of the plot in this frequency range is far from being vertical. In the same way, it can be seen that the real part of the impedance is strongly frequency dependent: the low frequency resistance (8 mHz) is 34 mΩ, that is to say there is a factor of 3 between the low frequency value of the resistance (at 8 mHz) and the high frequency value

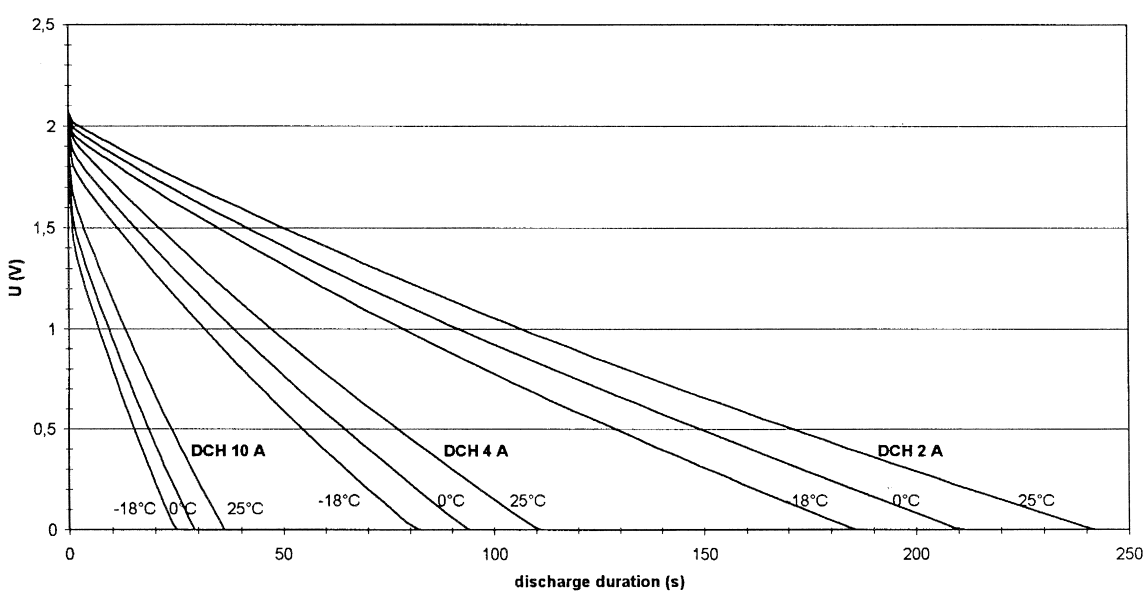

Fig. 4. Constant current discharge at different current (2, 4 and 10 A) and different temperatures (25, 0 and −18°C) for the SC#1 cell. Test sequence: charge $+I$ until 2.15 V/10 s rest/discharge $-I$ until 0 V.

Table 2
Characteristics of the SC#1 cell during discharge at different current and different temperatures

Temperature (°C)	I (A)	V_{dis} (V)	C (F)	R_{cycl} (mΩ)	$R_{1000\ Hz}$ (mΩ)
0°C	2	2.01	211	29	12.8
	4	1.89	202	27.5	12.8
	10	1.59	199	25.5	12.8
−18°C	2	2.04	190	40	16.6
	4	1.97	182	36	16.6
	10	1.79	182	32	16.6

(at 2 kHz). This can be explained assuming the electrolyte penetration into the porous structure of the electrode, which is here observed between 2 kHz and 100 mHz. To minimize this factor, the thickness of the electrodes must be decreased.

3.2.3. Low temperature cycling

SC#1 was cycled at different temperatures. Fig. 4 presents the cycling curves obtained at different currents (2, 4 and 10 A) and at different temperatures (25, 0 and −18°C). In these experiments, the supercapacitor is charged under constant current up to 2.15 V. The current is then turned off for 10 s before discharge is performed. Table 2 gives the characteristics of the cell. The capacitance decreases when the temperature decreases from 25 to −18°C, with a loss which is approximately 20%. A slight recrystallization of the salt into the pores of the electrodes could explain this decrease in the capacitance. An interesting observation is at low temperature, where the resistance at −18°C is less than doubled as compared to 25°C. The power loss at low temperature is not limiting the supercapacitor performances.

Table 3
Characteristics of the supercapacitor SC#2 during cycling at constant current (T = 25°C)

I (A)	V_{dis} (V)	C (F)	R_{cycl} (mΩ)	R_{ESR} (MΩ)
2	2.1	272	17.5	11
4	2.06	264	17	11
10	1.8	255	16	11

The tests carried out on SC#1 show that the electrode thickness must be decreased in order to limit the frequency-dependence of the resistance and to increase the volumetric capacitance. In the same way, the resistance of the cell must be decreased.

3.3. SC#2 cell tests

Taking into account the conclusions drawn from the previous experiments, a second supercapacitor was assembled. The thickness of the electrodes was decreased by modifying the amount of active material and a 24-electrode cell (SC#2) was assembled in a prismatic way (12 electrodes for each polarity). The composition of the electrodes was 80% activated carbon, 15% electronic conductor, 5% PTFE, the latter replacing CMC in order to improve the mechanical properties of the electrodes.

3.3.1. Constant current cycling

Fig. 5 presents the cycling of SC#2 between 0 and 2.1 V at 4 A (T = 25°C), and Table 3 lists the characteristics of the supercapacitor at different currents (2, 4 and 10 A). The low current test on SC#2 was performed on a Biologic VMP which is a multi-channel battery tester. The VMP tester is capable of measuring voltage differences of

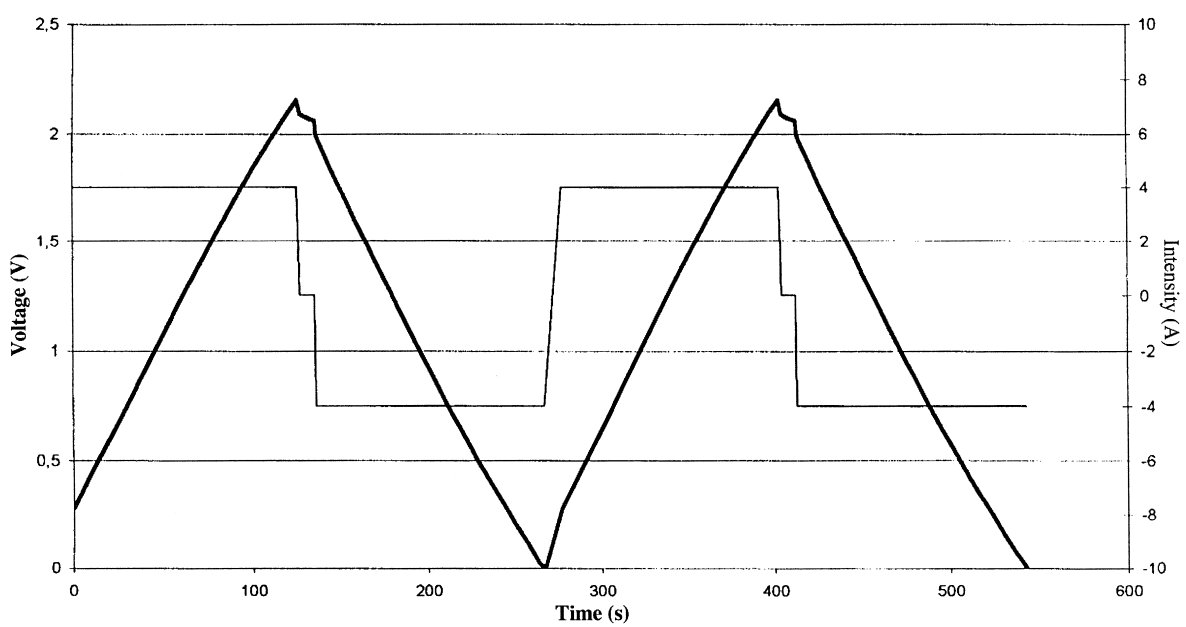

Fig. 5. Constant current charge–discharge cycles for the SC#2 cell. I = 4 A. Test sequence: charge $+I$ until 2.15 V/10 s rest/discharge $-I$ until 0 V.

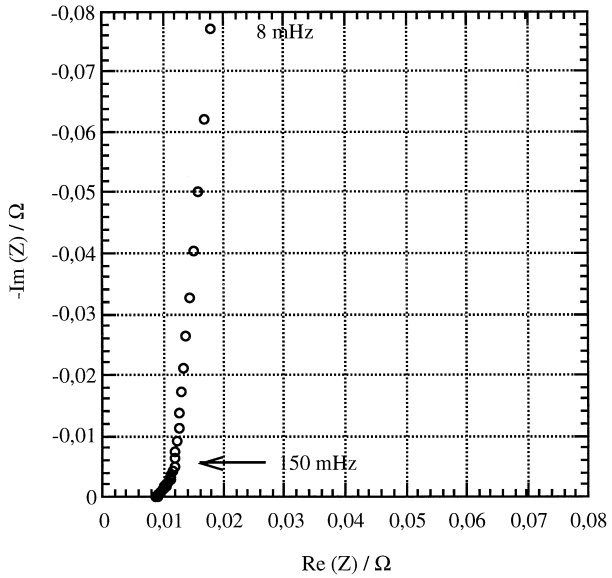

Fig. 6. Impedance spectrum of the SC#2 cell, between 2 kHz and 8 mHz.

a fraction of a mV and of taking data at rates of up to 50 Hz, which was particularly useful in determining the resistance of the cell noted as R_{ESR} in Table 3.

The capacitance of the cell is 272 F at 2 A. Once again, the capacitance loss for the different rates of discharge between 2 and 10 A is less than 6.5%. This capacitance corresponds to a volumetric capacitance of 23.5 F/cm^3 per electrode. This value is higher than that obtained for SC#1. The resistance measured during cycling at 2 A is 10 mΩ, which corresponds to a specific surface resistance of 8 Ω cm^2.

Table 4
Characteristics of the SC#2 cell during discharge at different current and different temperatures

Temperature (°C)	I (A)	V_{dis} (V)	C (F)	R_{cycl} (mΩ)	R_{ESR} (MΩ)
0°C	2	2.10	248	19	11.8
	4	2.07	239	18	11.8
	10	1.96	232	17	11.8
−18°C	2	2.10	229	20	12.6
	4	2.06	220	19	12.6
	10	1.96	216	18	12.6

3.3.2. Impedance measurements

The impedance spectrum of the 24-electrode cell SC#2 in the 2 kHz and 8 mHz impedance range is presented in Fig. 6. The knee frequency appears at 150 mHz, a value higher than that observed for SC#1. The behavior of the supercapacitor below frequencies of 150 mHz tends to the be purely capacitive. The real part of the impedance is less frequency-dependent than the one measured for SC#1. There is a factor of 2.3 between the low frequency value of the resistance (at 8 mHz) and the high frequency value (at 2 kHz). The smaller thickness of the electrode has decreased the frequency-dependence of the resistance significantly. A hypothesis can be made: the penetration of the electrolyte into the porous structure of the electrode is more rapid, thus leading to a decrease in the resistance.

3.3.3. Low temperature cycling

SC#2 was cycled at different temperatures, under different constant currents. Fig. 7 presents the obtained cycling curves. Tests were carried out in the same way as for SC#1. Table 4 lists the characteristics of the cell during discharge. The capacitance loss between 25 and −18°C is

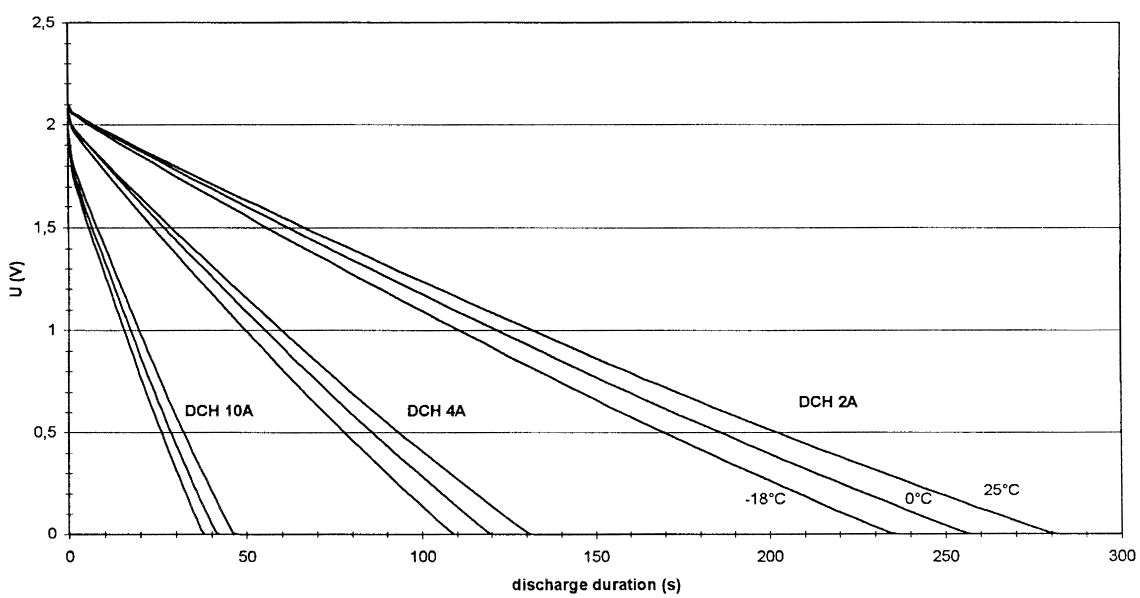

Fig. 7. Constant current discharge at different current (2, 4 and 10 A) and different temperatures (25, 0 and −18°C) for the SC#2 cell. Test sequence: charge $+I$ until 2.15 V/10 s rest/discharge $-I$ until 0 V.

Fig. 8. Supercapacitor SC#3. Weight of the supercapacitor: 134 g, volume: 100 cm^3.

16%, less than that observed for SC#1. The good behavior of the cell at low temperatures is confirmed by the small change in resistance. There is a factor less than 1.5 between the resistance at −18°C and the one measured at 25°C. The same conclusions as for SC#1 can be drawn from these measurements: the loss of power when operating at temperature down to −18°C is small.

Table 5
Characteristics of the supercapacitor SC#3 during cycling at constant current ($T = 25$°C). Weight of the supercapacitor: 134 g

I (A)	V_{dis} (V)	C (F)	R_{cycl} (mΩ)	R_{ESR} (mΩ)	P_{max} (kW/kg)	E_{max} (W h/kg)
2	2.13	294	17		1.1	1.4
4	2.12	294	16	8	1.1	1.4
10	2.12	294	15		1.1	1.4

The study of the 24-electrode cell SC#2 has shown that improvements have been obtained as compared to SC#1. However, the volumetric capacitance and the specific surface resistance of the cell must be improved. One solution may be to increase the number of electrodes to decrease the resistance of the cell, while at the same the same time taking care of the volumetric capacitance by adjusting the amount of active material in the electrodes.

3.4. SC#3 cell tests

A third supercapacitor SC#3 was assembled taking into account the previous conclusions, and is presented in Fig. 8. The composition of the electrodes was the following: 95% activated carbon, 5% PTFE. Previous tests carried out on smaller cells with this composition showed that good electronic properties in such electrodes could be obtained by modification of the manufacturing process. The mechanical properties of these electrodes were as good as for SC#2. A 28-electrode cell was assembled.

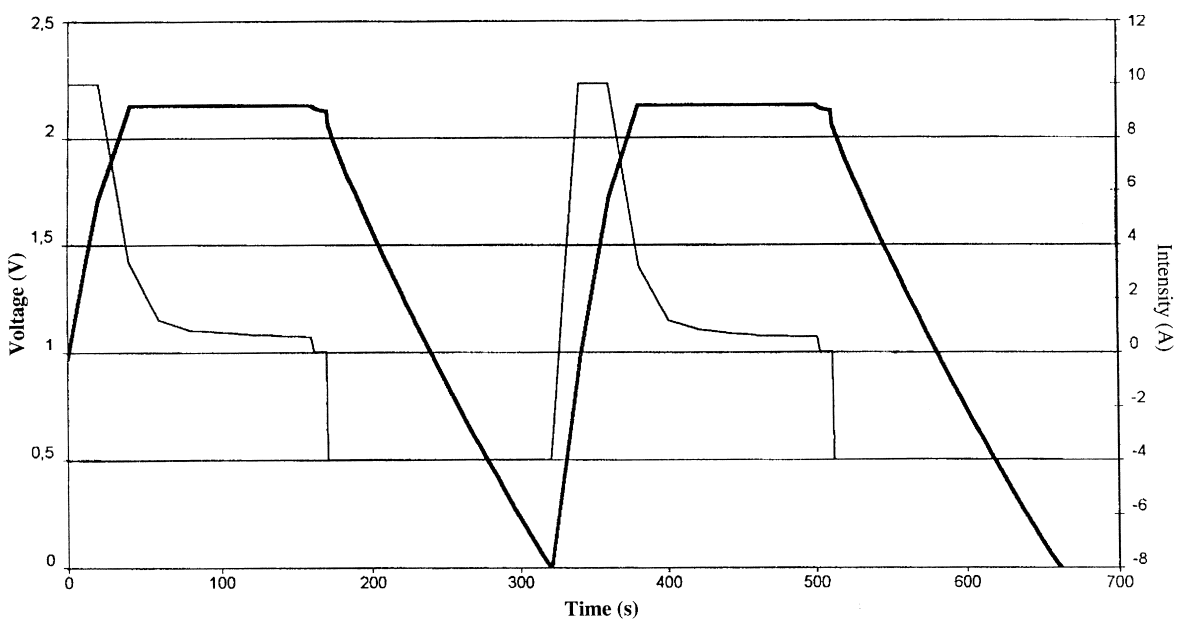

Fig. 9. Constant current charge–discharge cycles for the SC#3 cell. $I = 4$ A.

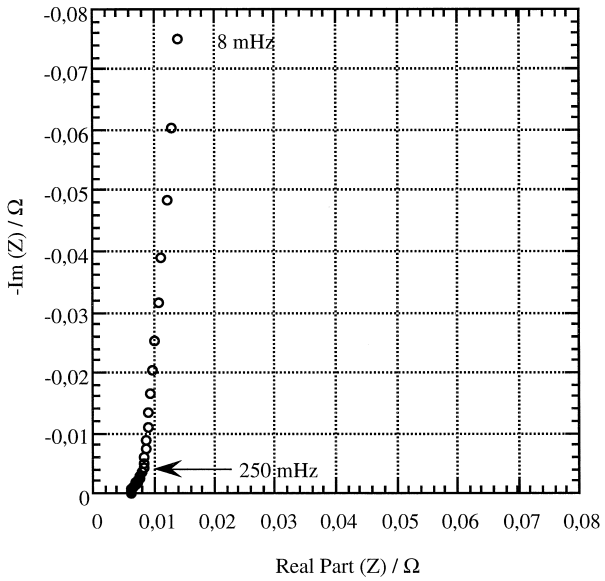

Fig. 10. Impedance spectrum of the SC#3 cell, between 2 kHz and 8 mHz.

3.4.1. Constant current cycling

Fig. 9 represents the cycling of SC#3 between 0 and 2.1 V at 4 A ($T = 25$°C) and Table 5 gives the characteristics of the cell during the tests. The capacitance of the cell remains constant during discharge at different currents, i.e., at a value of 294 F. This is an interesting result which leads to a volumetric capacitance of 25.3 F/cm^3 per electrode (including the current collector). The resistance of the cell during cycling, R_{ESR} is now equal to 8 mΩ, leading to a specific surface resistance of 6.5 Ω cm^2. This value makes the supercapacitor to reach a maximum specific power value of 1.1 kW/kg and a maximum specific energy value of 1.4 W h/kg (based on the total weight of the cell). The time constant is now equal to 2.3 s, which is now compatible with power applications.

3.4.2. Impedance measurements

The impedance spectrum of the 28-electrode cell SC#3 is represented in Fig. 10. The range of frequency is 2 kHz–8 mHz. The knee frequency is 250 mHz. This value is higher than the ones previously obtained. Below 250 mHz the frequency-dependence of the resistance is weak and the supercapacitor behavior tends to be purely capacitive. At 2 kHz, the value of R is 7 mΩ, and reaches 14 mΩ at 8 mHz. There is a factor of two between the low and the high frequency value of R. Therefore, the frequency-dependence of the real part of the impedance has been limited. The decrease in the thickness of the electrodes (and the increase in the number of electrodes) associated with the change in the active material composition explains this result.

3.4.3. Low temperature cycling

SC#3 was cycled at different temperatures, under different constant currents, in the same manner as SC#1 and SC#2. Fig. 11 presents the discharge curves at different temperatures and different currents. Characteristics of SC#3 measured during discharge are given in Table 6. Temperature varies from −18°C to 25°C and the discharge currents are in the range of 2–10 A. In this temperature range, the capacitance loss for this cell was 18%, which is a value intermediate between the losses found previously (20–16%). The loss of maximum specific energy reaches

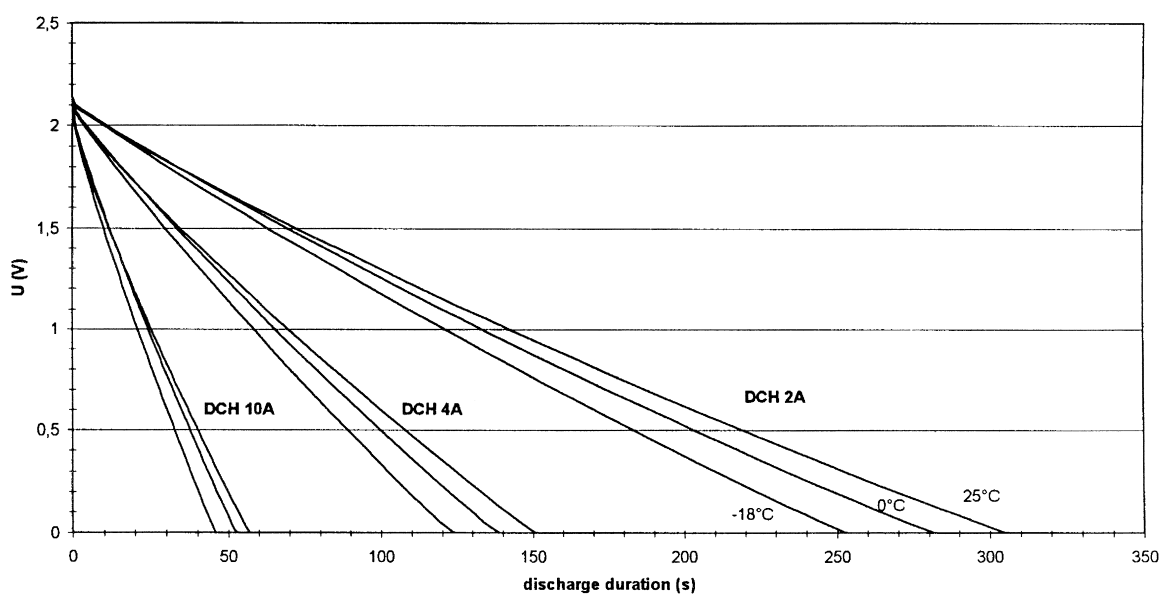

Fig. 11. Constant current discharge at different current (2, 4 and 10 A) and different temperatures (25, 0 and −18°C) for the SC#3 cell. Test sequence: charge $+I$ until 2.15 V/10 s rest/discharge $-I$ until 0 V.

Table 6
Characteristics of the SC#3 cell during discharge at different current and different temperatures

Temperature (°C)	I (A)	V_{dis} (V)	C (F)	R_{cycl} (mΩ)	P_{max} (kW/kg)	E_{max} (W h/kg)	R_{ESR} (mΩ)
0°C	2	2.14	264	18	0.930	1.260	9.2
	4	2.14	271	16	0.930	1.260	9.2
	10	2.14	266	16	0.930	1.260	9.2
−18°C	2	2.14	239	20	0.820	1.130	10.5
	4	2.14	239	19	0.820	1.130	10.5
	10	2.14	239	18	0.820	1.130	10.5

24% when the temperature changes from 25°C to −18°C. An interesting observation is the change in the resistance with respect to the temperature. From 25 to 0°C, R_{ESR} increases by 15%, that is to say, the resistance is multiplied by a factor of 1.15. This favorable behavior leads to a maximum specific power value P_{max} of 0.930 kW/kg at 0°C. The value of P_{max} decreases to 0.830 kW/kg when the temperature decreases down to −18°C, which corresponds to a 16% increase in resistance. As compared to 25°C, the loss of specific power when operating at −18°C is only 25%. Characteristics obtained for SC#3 make it interesting for operating at low temperatures.

4. Conclusions

This study concerns the fabrication of low-cost prismatic carbon/carbon power supercapacitors. Three 2 V-cells were assembled and tested. The composition of the active material and the electrode thickness were adapted in order to decrease the resistance of the supercapacitors and to increase the volumetric capacitance. A 28-electrode cell containing electrodes made up of 95% activated carbon/5% PTFE on nickel foam gave interesting results. A maximum specific power of 1.1 kW/kg and a maximum specific energy of 1.4 W h/kg (based on the total weight of the cell) were reached at 25°C. The cycling at different temperatures has confirmed the supercapacitor behavior between 25 and −18°C. In this temperature range, the loss of the maximum specific energy reached 24% while the loss of the maximum specific power was 25%. The time constant of the cell was 2.3 s, i.e., a value compatible with power applications. The volumetric capacitance of the cell was calculated as 25 F/cm^3 per electrode (including current collector). Future work will consist in decreasing the separator thickness, which is now higher than 100 μm, and test a new electrode composition which has recently given good results which respect to resistance and volumetric capacitance on smaller cells.

Acknowledgements

The authors from the CEAC company would like to thank the Ministère de l'Education Nationale, de la Recherche et de la Technologie for financial support of this work. The authors from the CNAM Laboratory would like to thank the Délégation Générale pour l'Armement and the CEAC company for financial support of this work.

References

[1] X. Andrieu, J.F. Fauvarque, Supercapacitors for telecommunication applications, 15th International Telecommunication Energy Conference (Intelec) 93, Paris, September 1993.
[2] P. Konsweil, O. Scchmid, A. Loffler, Proceedings of The 7th International Seminar on Double Layer Capacitors and Similar Energy Storage Devices, Deerfield Beach, FL, December 8–10, 1997.
[3] J. Farahmandi, D. Gideon, Proceedings of The 6th International Seminar on Double Layer Capacitors and Similar Energy Storage Devices, Deerfield Beach, FL, December 9–11, 1996.
[4] M.F. Rose, C. Johnson, T. Owens, B. Stephens, Journal of Power Sources 47 (1994) 303.
[5] I. Tanahashi, A. Yoshida, A. Nishino, Bull. Chem. Soc. Jpn. 63 (1990) 2755.
[6] J.P. Zheng, T.R. Jow, Journal of Electrochem. Soc. 142 (1995) L6.
[7] J.P. Ferraris, I.D. Brotherston, D.C. Loveday, Proceedings of The 38th Power Sources Conference, Cherry Hill, NJ, USA, 8–11 June 1998.
[8] L. Bonnefoi, P. Simon, J.F. Fauvarque, C. Sarrazin, A. Dugast, Proceedings of The 38th Power Sources Conference, Cherry Hill, NJ, USA, 8–11 June 1998.
[9] B.E. Conway, W. Pell, Proceedings of the 7th International Seminar on Double Layer Capacitors and Similar Energy Storage Devices, Deerfield Beach, FL, December 8–10, 1997.